

Electronic Supplementary Information

For

Novel microfibrinous composite bed reactor: high efficiency H₂ production from NH₃ with potential for portable fuel cell power supplies

Yong Lu,* Hong Wang, Ye Liu, Qingsong Xue, Li Chen and Mingyuan He

Shanghai Key Laboratory of Green Chemistry and Chemical Processes, Department of Chemistry, East China Normal University, Shanghai 200062, China.

Tel./Fax: (86) 21 6223-3424; E-mail: ylu@chem.ecnu.edu.cn

Table S1

Effect of REO loading on the performance of microfibrous entrapped Ni/REO-Al₂O₃ catalyst composite for NH₃ decomposition with a 72sccm feed rate at various reaction temperatures in a 0.5cm³ bed ^a

REO loading ^b (wt%)	Ni particle size ^c (<i>d</i> , nm)	Ni dispersion ^d (<i>D</i> , %)	NH ₃ conversion at various reaction temperature (mol%)		
			500°C	550 °C	600 °C
0	21	4.8	--	--	90.0
5 (CeO ₂)	22	4.5	52.2	87.9	99.2
10 (CeO ₂)	25	4.0	56.8	90.0	99.99
15 (CeO ₂)	25	4.0	57.0	89.7	99.99
10 (La ₂ O ₃)	23	4.3	48.3	84.1	98.2

^a The Ni loading of 10wt% was constant; the catalytic reaction beds were all reduced at 500°C for 2h in a H₂ flow of 50 sccm prior to NH₃ decomposition. ^b Samples in each step were calcined in air for 2h at 450°C for loading CeO₂ additives but at 250°C for loading Ni. ^c The estimate of Ni particle size (*d*) was approximated by the Scherrer formula on the basis of Ni(111) diffraction line. ^d The nickel dispersion (*D*) was estimated by assuming *d* (nm) = 1/*D*.

Table S2

Effect of Ni loading on the performance of microfibrous entrapped Ni/CeO₂-Al₂O₃ catalyst composite for NH₃ decomposition with a 72sccm feed rate at various reaction temperatures in a 0.5cm³ bed ^a

Ni loading ^b (wt%)	Ni particle size ^c (<i>d</i> , nm)	Ni dispersion ^d (<i>D</i> , %)	NH ₃ conversion at various reaction temperature (mol%)			
			500°C	550 °C	600 °C	650 °C
5	15	6.7	36.0	71.0	95.5	99.3
10	25	4.0	56.8	90.0	99.99	>99.99
15	37	2.7	49.4	84.4	98.3	99.8

^a The CeO₂ loading of 10wt% was constant; the catalytic reaction beds were all reduced at 500°C for 2h in a H₂ flow of 50sccm prior to NH₃ decomposition. ^b Samples in each step were calcined in air for 2h at 450°C for loading CeO₂ additives but at 250°C for loading Ni. ^c The estimate of Ni particle size (*d*) was approximated by the Scherrer formula on the basis of Ni(111) diffraction line. ^d The nickel dispersion (*D*) was estimated by assuming *d* (nm) = 1/*D*.

Table S3

Effect of calcination temperature in the step (1) of loading CeO₂ on the performance of microfibrinous entrapped Ni/CeO₂-Al₂O₃ catalyst composite for NH₃ decomposition with a 72sccm feed rate at various reaction temperatures in a 0.5cm³ bed ^a

Calcination temp. in step of loading CeO ₂ ^b (°C)	NH ₃ conv. at various reaction temp. (mol%)		
	500°C	550 °C	600 °C
250	54.7	87.7	99.1
450	56.8	90.0	99.99
550	50.1	75.0	93.9

^a The constant loading of 10wt% was used for both CeO₂ additive and Ni; the catalytic reaction beds were all reduced at 500°C for 2h in a H₂ flow of 50sccm prior to NH₃ decomposition. ^b In step of loading CeO₂, impregnated samples were calcined in air at appointed temperatures for 2h; after subsequently loading Ni by IWI with Ni(NO₃)₂·6H₂O, the catalyst samples were calcined in air at a fixed temperature of 250°C for 2h.

Table S4

Effect of calcination temperature in the step (2) of loading Ni on the performance of microfibrinous entrapped Ni/CeO₂-Al₂O₃ catalyst composite for NH₃ decomposition with a 72sccm feed rate at various reaction temperatures in a 0.5cm³ bed ^a

Calcination temp. in step of loading Ni ^b (°C)	NH ₃ conv. at various reaction temp. (mol%)		
	500°C	550 °C	600 °C
250	56.8	90.0	99.99
350	40.6	77.6	96.8
450	37.5	75.4	96.0
550	35.3	70.7	94.4

^a The constant loading of 10wt% was used for both CeO₂ additive and Ni; the catalytic reaction beds were all reduced at 500°C for 2h in a H₂ flow of 50 sccm prior to NH₃ decomposition. ^b In step of loading CeO₂, impregnated samples were calcined in air at a fixed temperature of 450°C for 2h; after subsequently loading Ni by IWI with Ni(NO₃)₂·6H₂O, the catalyst samples were calcined in air at appointed temperatures for 2h.

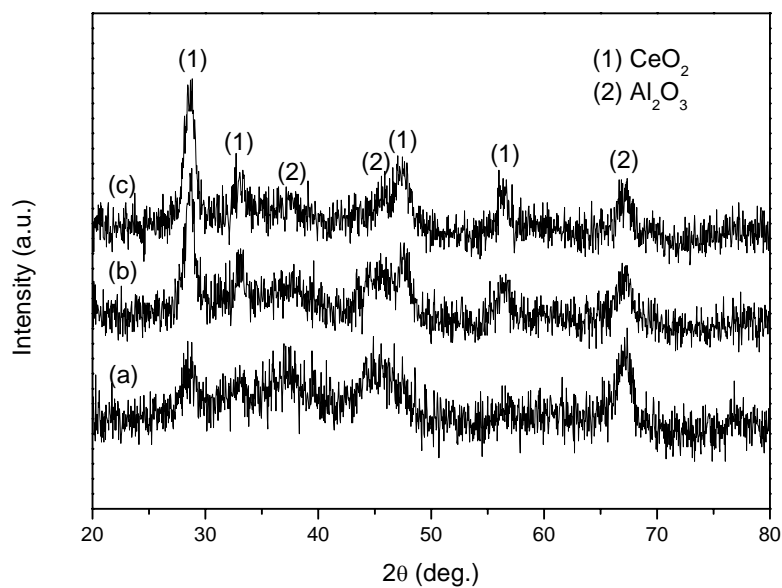


Fig. S1 XRD patterns of CeO₂-Al₂O₃ support samples with CeO₂ loading of (a) 5wt%, (b) 10wt%, and (c) 15wt%. CeO₂-Al₂O₃ support particulates were the same samples as in Table S1 that just were loaded with CeO₂ but not with Ni, and were collected by disclosing the microfibrinous network for XRD experiment.

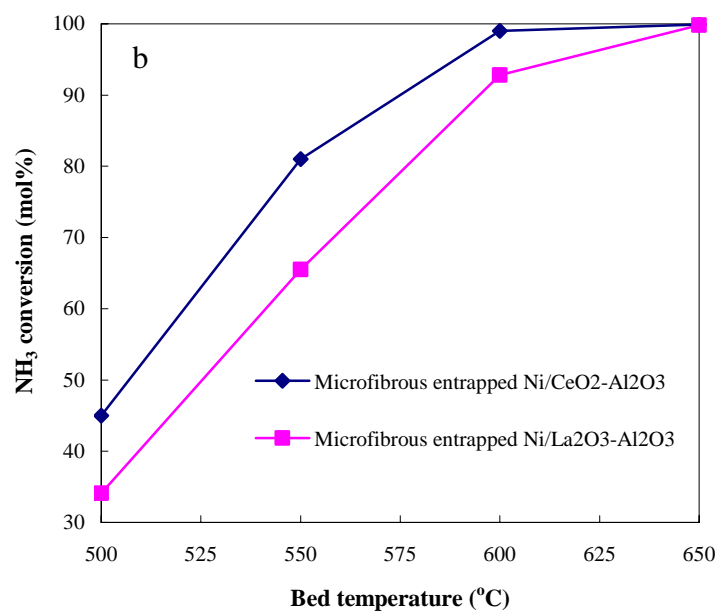
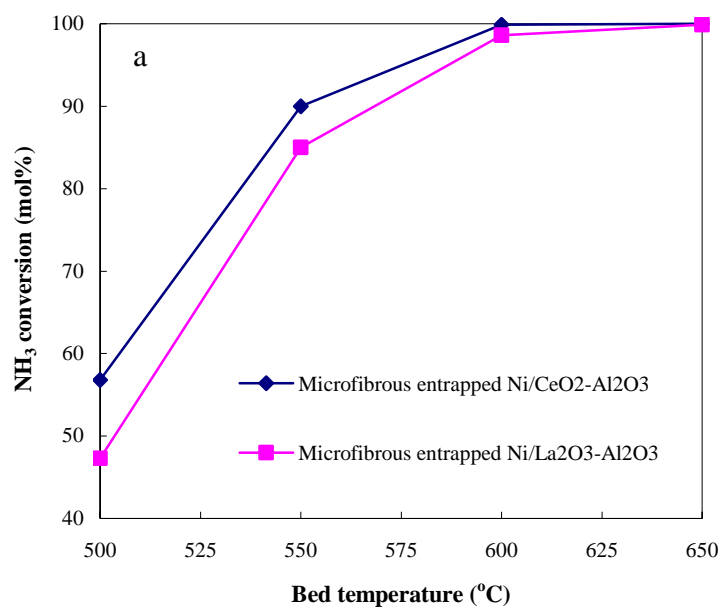


Fig. S2 NH₃ conversion over CeO₂- and La₂O₃-promoted microfibrous entrapped Ni/Al₂O₃ catalyst composites at various bed temperatures in bed volume of 0.5ml with NH₃ feed rate of (a) 72sccm and (b) 145sccm, respectively.

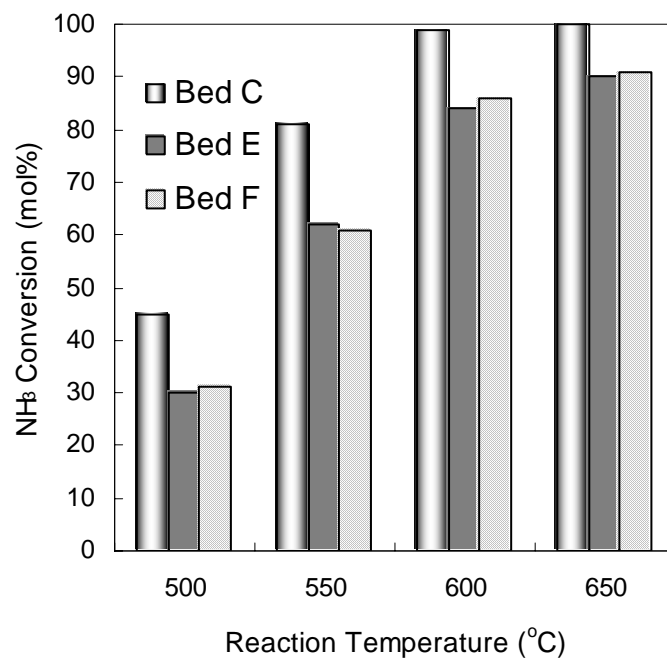


Fig. S3 Comparison of the reactivity of bed C with beds E and F at various reaction temperatures with a 145sccm NH₃ feed gas rate. See *footnotes* in Table 2 of the paper for the descriptions of beds C, E and F.

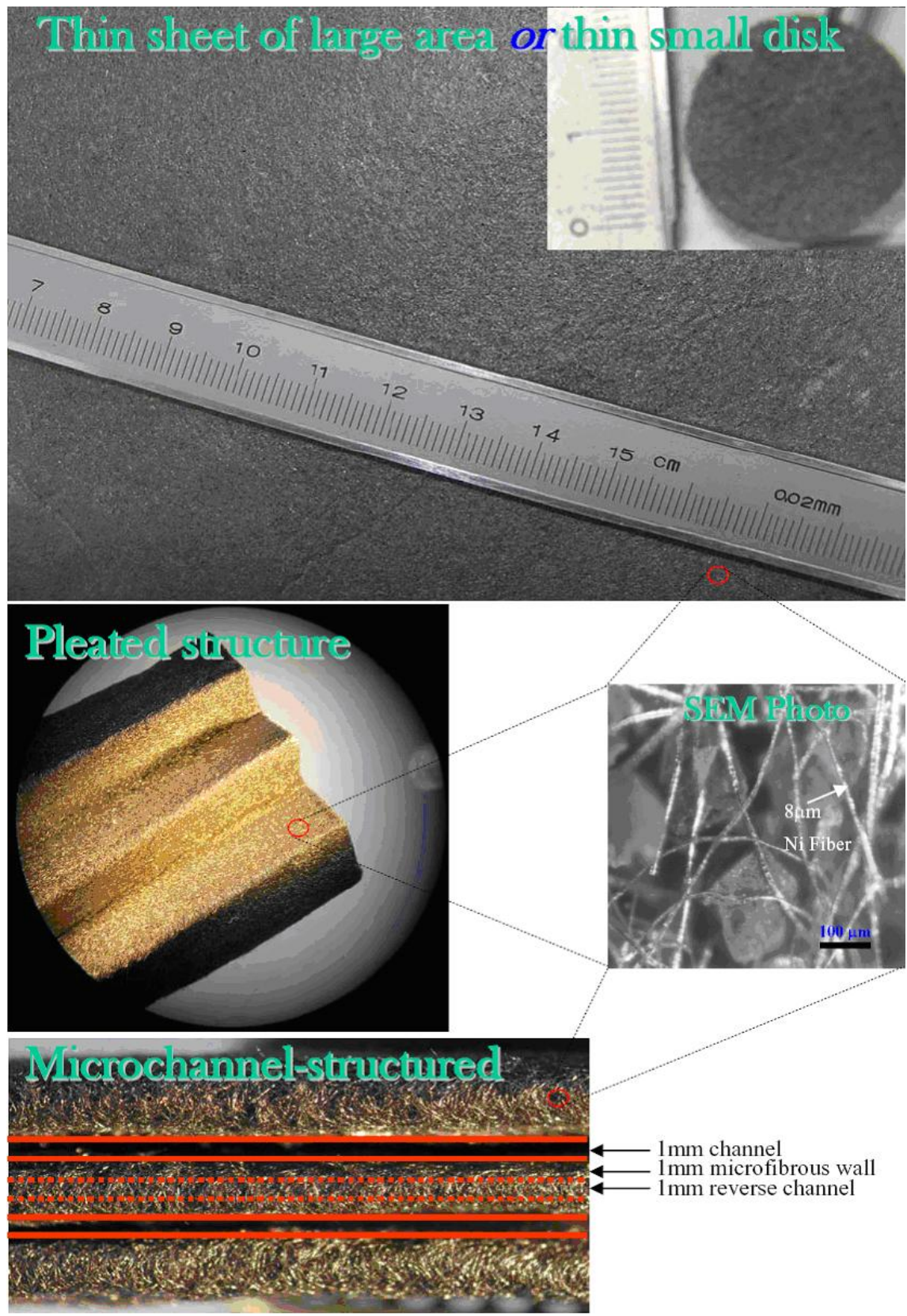


Fig. S4 Unique form factors of microfibrous media with micron-sized particulates using 8 μ m diameter nickel microfibers.

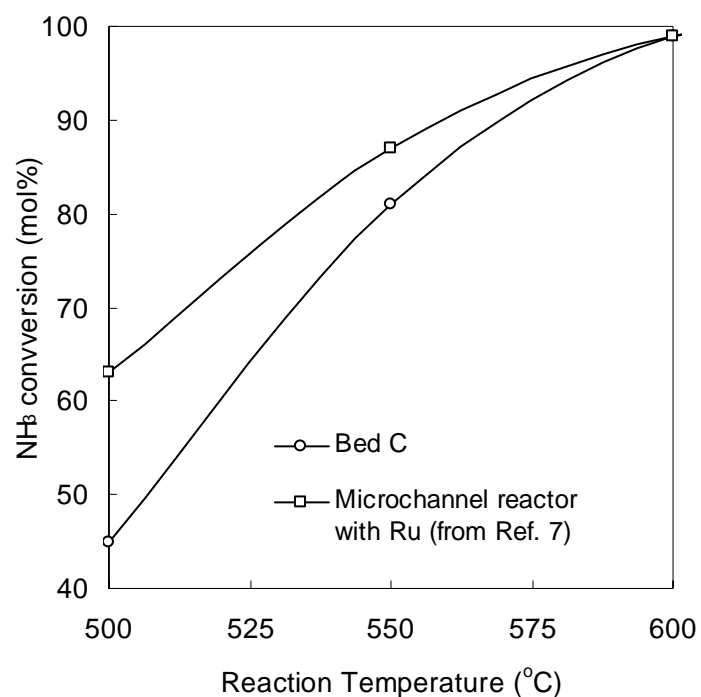


Fig. S5 Comparison of the performance of bed C with the state-of-the-art microchannel reactor with Ru for NH_3 decomposition at various reaction temperatures with a 145 sccm NH_3 feed gas rate. See *footnotes* in Table 2 of the paper for the descriptions of bed C.

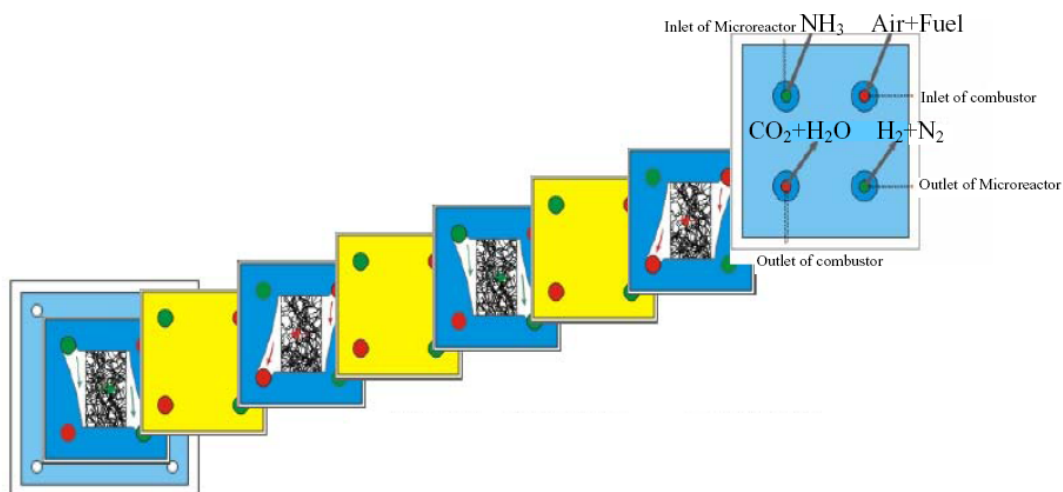


Fig. S6 Proposed model for a small plate-type reactor system with integrated microcombustor design based on our microfibrinous catalyst composite for NH_3 decomposition to produce *CO-free* H_2 .